

Photoresponsive Self-Assembly and Self-Organization of Hydrogen-Bonded Supramolecular Tapes

Shiki Yagai,* Tomoyuki Iwashima, Keiki Kishikawa, Shoichiro Nakahara, Takashi Karatsu, and Akihide Kitamura*[a]

Abstract: Self-assembling building blocks that are readily functionalizable and capable of achieving programmed hierarchical organization have enabled us to create various functional nanomaterials. We have previously demonstrated that *N,N*-disubstituted 4,6-diaminopyrimidin-2(1*H*)-one (DAP), a guanine–cytosine hybridized molecule, is a versatile building block for the creation of tapelike supramolecular polymer species in solution. In the current study, DAP was functionalized with

azobenzene side chains. ¹H NMR, UV/Vis, and dynamic light scattering studies confirmed the presence of nanometer-scale tapelike supramolecular polymers in alkane solvents at micromolar regimes. At higher concentrations (millimolar regimes), the supramolecular polymers hierarchically organized into

Keywords: azobenzene • organogels • photoisomerization • self-assembly • supramolecular chemistry

lamellar superstructures to form organogels, as shown by X-ray diffraction and polarized optical microscopy. Remarkably, the azobenzene side chains are photoisomerizable even in the supramolecular polymers, owing to their loosely packed state supported by the rigid hydrogen-bonded scaffold, enabling us to establish photocontrollable supramolecular polymerization and higher order organization of the tapelike supramolecular polymers into lamellar superstructures.

Introduction

Supramolecular polymers are fascinating materials exhibiting self-repairing and stimuli-responsive properties arising from their reversible natures.^[1] A spontaneous chain-elongation process based on noncovalent interactions permits the polymerization of supramolecular building blocks possessing chemically labile functional groups under ambient conditions, thus paving the way for the preparation of polymeric materials featuring various functional side chains such as optically and electronically active dyes.^[2] These supramolecular polymers would thus be expected to exhibit novel photochemical or electrochemical activities, with the individual properties of the chromophoric units being amplified at the supramolecular levels.

DNA base-type multiple hydrogen-bonding interactions^[3] should be the most beneficial noncovalent glue for the crea-

tion of supramolecular polymers, due to their high directionality and selectivity.^[4,5] Another attractive feature of the use of this type of noncovalent interaction is that the hydrogen-bonded planes created by heterocyclic aromatic compounds are capable of hierarchically organizing through π – π stacking and van der Waals interactions to provide diverse mesoscopic assemblages such as columnar^[4e,6] and lamellar structures,^[7,8] depending on the shape of the primary hydrogen-bonded species. The resulting hierarchically organized mesoscopic assemblages often exist in a gel phase in the presence of appropriate solvents and a liquid crystalline mesophase in the bulk state. Such spontaneous formation of highly organized superstructures plays a pivotal role in the fabrication of organic materials requiring high levels of molecular anisotropy.

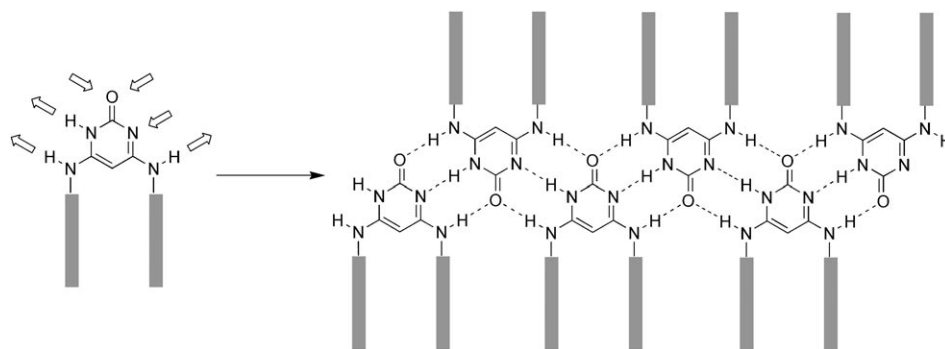
Functionalization of supramolecular building blocks with photoswitching molecules provides photoresponsive self-assemblies, which have recently attracted considerable attention.^[9,10] While most systems utilize morphological changes in photochromic chromophores to control inter- or intramolecular hydrogen-bonding interactions on the formation of supramolecular species, their application to control the hierarchical organization of supramolecular species is very rare. We recently reported photochemical control over the stacking of hydrogen-bonded cyclic oligomers (rosettes) through

[a] Dr. S. Yagai, T. Iwashima, Prof. Dr. K. Kishikawa, S. Nakahara, Prof. Dr. T. Karatsu, Prof. Dr. A. Kitamura
Department of Applied Chemistry and Biotechnology
Faculty of Engineering, Chiba University, 1–33 Yayoi-cho
Inage-ku, Chiba 263–8522 (Japan)
Fax: (+81)43-290-3039
E-mail: yagai@faculty.chiba-u.jp

the use of photoisomerization of azobenzene chromophores.^[6] As another example of photoresponsive hierarchical organizations of supramolecular species, here we report photoresponsive tapelike supramolecular polymers based on multiple hydrogen-bonding interactions, which can hierarchically organize into lamellar superstructures.

Selective formation of linear, tapelike supramolecular polymers (supramolecular tapes) is of profound importance for the creation of rigid nanostructures exhibiting high molecular anisotropy. Multiple hydrogen-bonding interactions represent a convenient tool for the construction of such tapelike assemblies, as exemplified by complementary melamine-barbiturate/cyanurate systems.^[11] Gottarelli et al.^[7] and Kato et al.^[8] have reported supramolecular tapes generated from guanine and folic acid derivatives, respectively. The planar and rigid structures of the supramolecular tapes eventually give rise to the formation of lamellar superstructures to form gels and (lyotropic) liquid crystalline mesophases. We recently reported the synthesis and the self-assembly of *N,N'*-disubstituted 4,6-diaminopyrimidin-2(1*H*)-ones (DAPs, see Figure 1) featuring donor–donor–acceptor (DDA) and acceptor–acceptor–donor (AAD) hydrogen-bonding arrays.^[12] These self-complementary guanine–cytosine hybridized supramolecular building blocks are based on 5-octyl-4,6-diaminopyrimidin-2(1*H*)-one, reported by Lehn et al. in 1992,^[13] but they can be functionalized even more easily. DAP building blocks possessing long aliphatic chains have been shown to form robust supramolecular tapes in solution and in the solid state, so a lot of functionalized supramolecular tapes based on DAP building blocks are available.

In this work the photoresponsive supramolecular tape was constructed from azobenzene-pendent DAP building blocks (Scheme 1). Through photoisomerization of the pendent azobenzene moieties, both supramolecular polymeri-

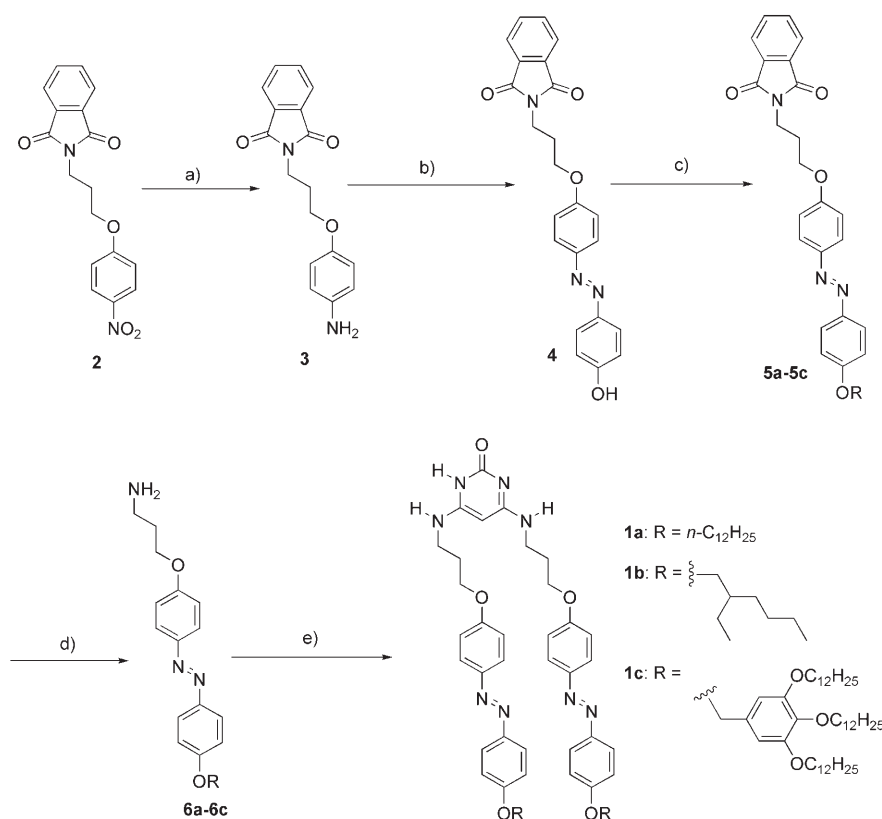


Scheme 1. Supramolecular polymerization of *N,N'*-disubstituted 4,6-diaminopyrimidin-2(1*H*)-one (DAP) units.

zation under dilute conditions and the hierarchical organization of the resulting supramolecular tapes into lamellar superstructures under concentrated conditions can be controlled by external light input.

Results and Discussion

Synthesis: We designed and synthesized azobenzene-functionalized DAPs **1** (Scheme 2) in which two photoresponsive azobenzene units tailed with solubilizing chains are attached to the 4- and 6-amino groups through propoxy linkers. An



Scheme 2. Synthesis of **1**. a) Pd/C, THF, H₂, 65°C; b) NaNO₂, aq. HCl, then phenol, NaOH, Na₂CO₃, H₂O; c) K₂CO₃, 1-bromododecane (for **1a**), 1-bromo-2-ethylhexane (for **1b**), or 3,4,5-tris(dodecan-1-yloxy)benzyl chloride (for **1c**), DMF, 65°C; d) Hydrazine monohydrate, EtOH; e) sodium 4,6-dichloropyrimidin-2(1*H*)-onate, dioxane, diisopropylethylamine, 105°C, 24 h.

attempt to introduce aminoazobenzene derivatives directly onto the DAP unit was hampered by the low reactivity of the aminoazobenzene derivatives in the nucleophilic substitution with 4,6-dichloropyrimidin-2(1*H*)-one. The key compound for the synthesis of **1** was the monoetherified 4,4'-dihydroxyazobenzene derivative **4**, which was prepared by the diazonium coupling of aniline **3**—possessing a phthalimide-protected ω-aminopropoxy group at its 4-position—with phenol. Etherification of the hydroxy group of **4** with the appropriate halogenated compound and subsequent removal of the phthalimide protecting group gave azobenzene derivatives **6a–c**, each possessing a reactive aliphatic amino group. Finally, compounds **6a–c** were treated with 4,6-dichloropyrimidin-2(1*H*)-one to give the crude DAP-azobenzene compounds **1a–1c**.

Compound **1c**, possessing tridodecyloxyphenyl groups, shows good solubility in organic solvents, allowing its purification by silica gel column chromatography. Compound **1a**, however, is almost insoluble in common organic solvents, whilst compound **1b** is soluble only in chlorinated solvents such as chloroform and dichloromethane with gentle heating, the solutions turning to gels on cooling. Because of their poor solubilities arising from supramolecular polymerization, **1a** and **1b** could not be isolated in the high purities necessary to allow detailed investigation into their self-aggregation and hierarchical organization. Study of self-aggregation was therefore carried out only for **1c**, which was characterized by ¹H NMR, FAB-MS, and elemental analysis.

Self-assembly: Compound **1c** is highly soluble in THF and chloroform and even in nonpolar alkane media such as hexane and cyclohexane. The ¹H NMR spectrum of **1c** dissolved in CDCl₃ (*c* = 5 × 10^{−3} M) is well resolved, indicating the molecularly dissolved state (Figure 1a). The azobenzene moieties are almost entirely *trans* (>99%) under ordinary conditions, as shown by the resonances of the aromatic protons. In contrast, the spectrum of a [D₁₂]cyclohexane solution (*c* = 5 × 10^{−3} M) is greatly broadened in all resonances, indicating the formation of extended polymeric species (Figure 1b). The spectrum recorded at 75°C is somewhat resolved yet still broadened, indicating the high stability of the supramolecular polymers (Figure 1c).

In dynamic light scattering (DLS) analyses of **1c** dissolved in THF and CHCl₃ at concentrations ranging from 1 × 10^{−5} to 6 × 10^{−3} M, no large particles with definitive scattering light intensity detectable by our DLS instrument were observable at room temperature, indicating the absence of large aggregated species. As expected from the ¹H NMR results, the cyclohexane solution of **1c** (*c* = 5 × 10^{−3} M) gave moderate scattering intensity in DLS analysis owing to the formation of polymeric species. The cumulative analysis of the autocorrelation function resulted in a broad distribution of the hydrodynamic diameter (*D_h*) centered at 50 nm, which reflects the polydisperse nature of the linear supramolecular polymers. If it is assumed that the observed *D_h* corresponds to the gyration diameter of the rigid supramolecular polymers, the average aggregation number of 70 is estimated

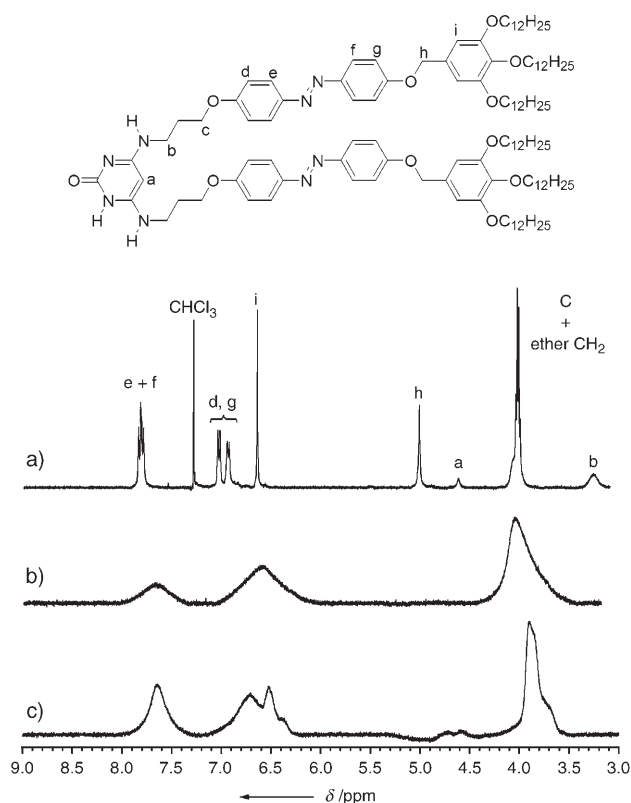


Figure 1. Parts of the ¹H NMR spectra of **1c** (*c* = 5 × 10^{−3} M) in a) CDCl₃ at 25 °C, and b) in [D₁₂]cyclohexane at 25 °C and c) at 75 °C.

from the length of molecular-modeled hexadecamer (11.5 nm), as shown below.

Compound **1c** is soluble on gentle heating even in heptane or higher alkane solvents. In these solvents the aggregation of **1c** was dramatically enhanced, DLS showing that the freshly prepared heptane solution contained aggregated species with the average *D_h* of 15 nm at a relatively low concentration (2 × 10^{−4} M) at 25 °C. Interestingly, the aggregates slowly grew, with a rate of roughly 8 nm h^{−1}, giving large aggregated species exceeding 150 nm after 12 h. The slow growth of the aggregates implies that the supramolecular polymerization of **1c** in heptane is driven not only by the strong DDA:AAD hydrogen bonding interaction (*K_{assoc}* reaches 10⁴ M^{−1} even in chloroform) but also by weak cohesive forces competing with the solvation by heptane (i.e., van der Waals and π–π stacking interactions). With increases in the concentration up to millimolar regimes, the solution became turbid with time with the propagation of filamentous aggregates as detailed below.

Figure 2a compares the UV/Vis absorption spectra of **1c** (*c* = 2 × 10^{−4} M) in THF (dashed line) and in heptane (solid line; the steady state obtained after the sample was left to stand for 12 h), corresponding to the monomeric and the aggregated states, respectively, whilst Figure 2b shows the spectra of a synthetic intermediate **5c** lacking the DAP hydrogen-bonding unit. The absorption band at λ_{max} = 280 nm is only observed in the spectra of **1c**, and is ascribable to the

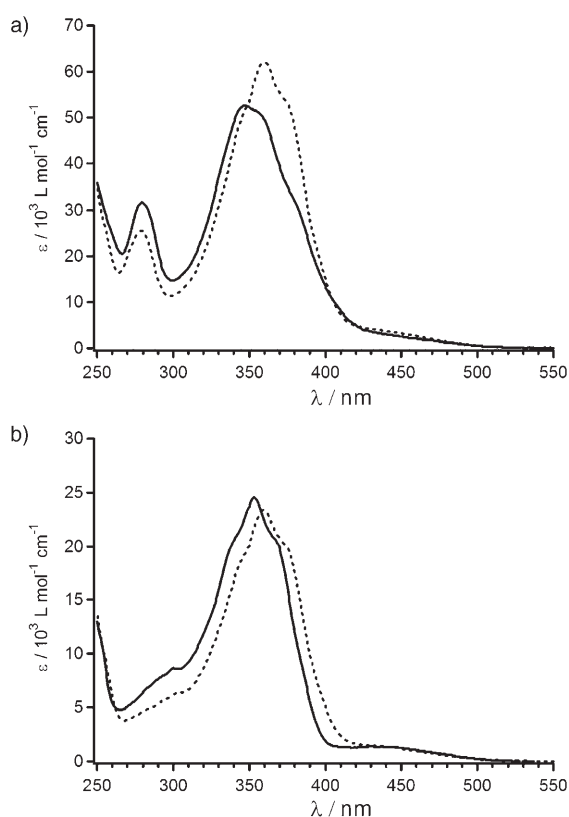


Figure 2. UV/Vis spectra of a) **1c** ($c = 2 \times 10^{-4} \text{ M}$), and b) **5c** ($c = 4 \times 10^{-4} \text{ M}$) in heptane (solid line) and THF (dashed line).

transition related to the DAP unit. The π - π transition band of the azobenzene moieties of **1c** in heptane is blue-shifted by 13 nm and less structured than that of the molecularly dissolved state in THF. Compound **5c**, without a DAP hydrogen-bonding unit, also shows a 6-nm hypsochromic shift with decreasing solvent polarity (Figure 2b), indicating that the solvent-dependent hypsochromic shift observed for **1c** involves inherent solvatochromism of the azobenzene chromophores. Therefore, the spectral change of the azobenzene chromophores of **1c** upon supramolecular polymerization is relatively small, in contrast with other azobenzene-based self-assemblies that are considerably stabilized by π - π stacking interactions,^[14] suggesting that the azobenzene chromophores in this supramolecular polymer are free of extended aggregation. This is clear evidence of the rigid nature of the DAP-based supramolecular polymer scaffold. The mismatch between the optimum π - π stacking distance (typically 3–4 Å) and the intervals of the nitrogen atoms of the amino groups bearing the azobenzene side chains (4.8–4.9 Å) may prevent extended π - π stacking of the azobenzene chromophores. A molecular modeling-derived hexadecamer of **1c** (MacroModel 9.0, MMFF force-field calculation), shown in Figure 3a, illustrates this situation: the azobenzene side chains were optimized as a partially overlapped dimeric state with adjacent chromophores. Such a loose molecular packing would provide the azobenzene chromophores with

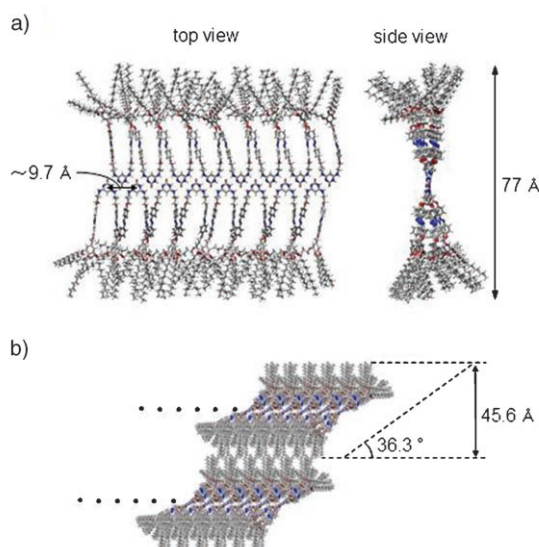


Figure 3. a) Molecular modeling structure of hexadecameric **1c**. b) Proposed packing motif for a supramolecular tape (side view).

the space prerequisite for photoisomerization within the supramolecular polymers.^[14]

Hierarchical organization: When heptane or higher alkane solutions of **1c** were allowed to stand, at a concentration of $1 \times 10^{-3} \text{ M}$, yellow filamentous precipitates started to appear within several hours. Optical microscopic observation of the precipitated solution revealed macroscopic fibers with sub-micrometer diameters and lengths over 10 μm (Figure 4a).

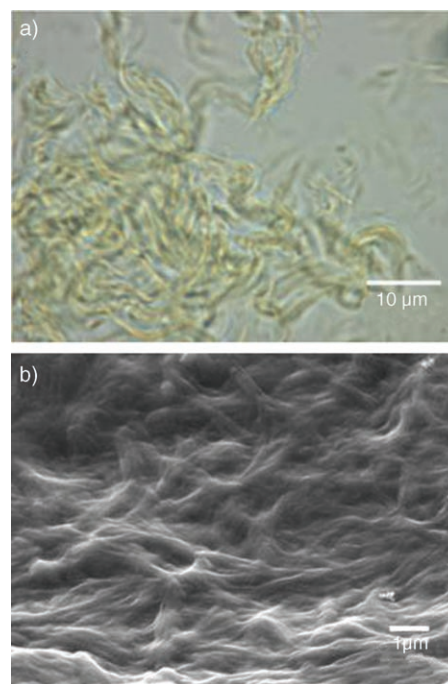


Figure 4. a) Optical microscopic image of a precipitated solution of **1c** in heptane. b) FE-SEM image of the dried precipitates of **1c**.

Observation of the freeze-dried precipitates by field-emission scanning electron microscopy (FE-SEM) also confirmed the presence of entangled fibrous entities with diameters of several hundred nanometers (Figure 4b).

Interestingly, use of more concentrated heptane or higher alkane solutions of **1c** resulted in the formation of two-dimensional sheet-like macroscopic entities on standing, as again observed by optical microscopy (Figure 5a) and FE-

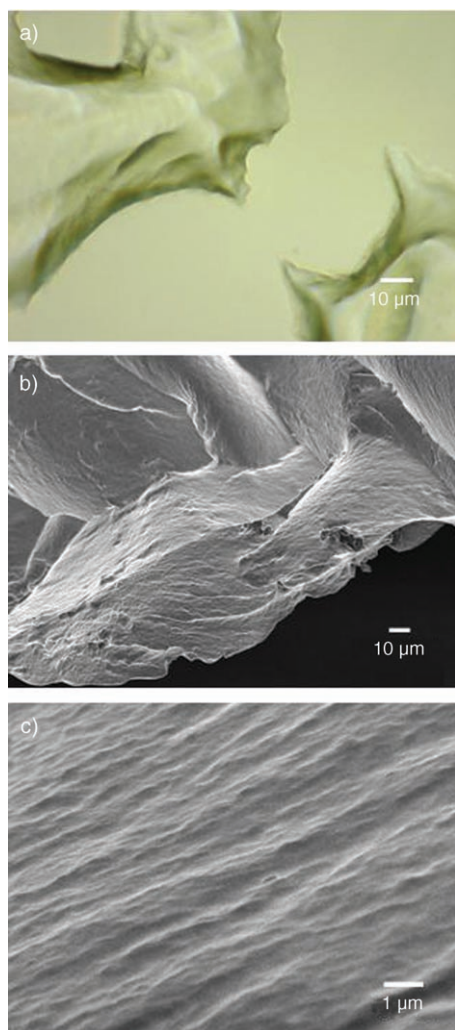


Figure 5. a) Optical microscopic image of the heptane gel of **1c**. b) FE-SEM image of the dried gel. c) Magnified image of b).

SEM after freeze-drying (Figure 5b). The resulting sheet-suspended liquids obtained after 12 h standing were opaque organogels that showed stability against gravitational flow (see Figure 10a and c).^[15] FE-SEM observation with high magnification revealed that the sheet was not composed of assembled fibers (Figure 5c). The supramolecular polymer of **1c** therefore hierarchically organizes into distinct macroscopic entities with variation of concentration.

The heptane organogel made up of the self-assembled sheet of **1c** was dried and analyzed by polarized optical microscopy (POM) and X-ray diffraction (XRD). The resulting

transparent film is strongly birefringent (inset in Figure 6a), indicating the presence of molecular anisotropy. The X-ray diffraction pattern of the film at room temperature is shown in Figure 6a. Most importantly, the weak Bragg diffraction

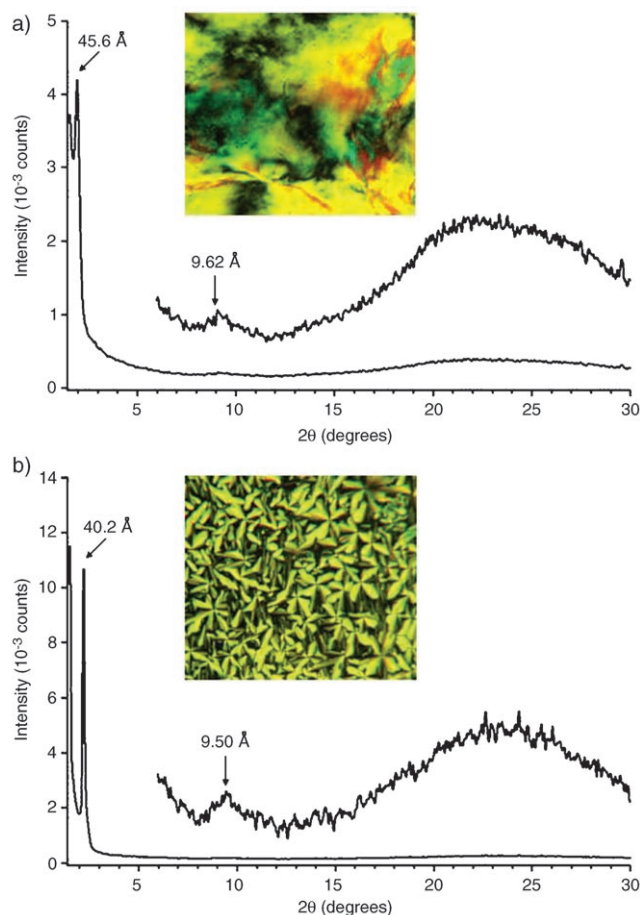


Figure 6. X-ray diffraction patterns and cross-polarized optical micrographs (insets) of self-assembled sheet of **1c** at a) room temperature, and b) 155 °C upon cooling from the isotropic liquid.

corresponding to a spacing of 9.62 Å matches very well with the periodic distance between the neighboring DAP units in the molecular modeling-derived tape (≈ 9.7 Å, side view in Figure 3a) as well as that in the crystal structure of 4,6-diamino-5-octylpyrimidin-2(1*H*)-one (9.68 Å) reported by Lehn et al.^[13] The broad diffuse halo in the wide-angle region indicates the liquid-like nature of the aliphatic tails. The sole intense peak observed in the small angle region suggests the presence of a lamellar structure with a spacing of 45.6 Å, which is commensurate neither with the width of the molecular modeling-derived tape of **1c** (ca. 77 Å, Figure 3a) nor with the molecular length of **1c** with extended alkyl chains (ca. 38 Å). Interdigitation of the aliphatic tails between the lamella is unlikely because of the steric crowding of aliphatic tails. Instead, tilted stacking ($\theta = 36.3^\circ$) of the tapes in the lamella, as shown in Figure 3b, is strongly suggested for a hierarchical structure. An almost identical lamellar structure was found for the cast film prepared from

the homogeneous cyclohexane solution of **1c** (data not shown). On the basis of these results, it can be suggested that the supramolecular tape of **1c** had two-dimensionally self-organized in the hydrocarbon media to form a lamellar superstructure in the self-assembled sheet.

The lamellar superstructure persisted up to isotropization (220 °C) as judged by the XRD analysis: no significant change in the sole observed diffraction peak at around 46 Å was observed with increasing temperature. In addition, no defined transition was detected by differential scanning calorimetry measurement until isotropization. Upon cooling slowly from the isotropic phase (1 °C min⁻¹), however, the presence of a columnar liquid crystalline mesophase was suggested from the focal conic textures observed between 92–220 °C (inset in Figure 6b). XRD analysis showed an intense peak corresponding to a spacing of 40.2 Å and a weak peak corresponding to a spacing of 9.50 Å. The presence of the latter peak corroborates the persistence of the supramolecular tape of **1c** in the mesophase. The former spacing is rather shorter than those observed for the lamellar structures, indicating the presence of a mesoscopic structure different from that observed before the isotropization. Combined with the focal conic texture, it is most likely that columns composed of several supramolecular tapes are arranged in two-dimensional ordering by micro-segregation^[16,17] due to the mismatched volume between the rigid aromatic core and the liquid-like aliphatic part mobile at high temperature.^[18] No definite assignment of the mesophase could be made, due to the absence of higher-order X-ray diffractions. Detailed investigation of the liquid crystalline behavior of DAP-based supramolecular tapes with the aid of DAP molecules possessing different optically active side chains is now underway.

Photoisomerization: The azobenzene moieties in both monomeric and aggregated **1c** undergo reversible photoisomerization on irradiation with UV light at around 350 nm (*trans*→*cis*) and subsequent irradiation with visible light at around 450 nm (*cis*→*trans*). Figure 7 shows the UV/Vis spectral changes of dilute THF (a) and heptane solutions (b) of **1c** ($c = 2 \times 10^{-5}$ M) upon irradiation with UV light. The *cis/trans* ratio in heptane at the photostationary state (PS) is 0.55, lower than that in THF (0.98). The lower *cis/trans* ratio in heptane is indicative of supramolecular polymerization of **1c** occurring at low concentrations. This was supported by a control experiment performed with synthetic intermediate **5c**, without the DAP unit, which showed a very high *cis/trans* ratio (0.99) upon UV irradiation even in heptane. The value of 0.55 for the *cis/trans* ratio corresponds to isomerization of one of the two azobenzene side chains of **1c** in the supramolecular tape.

To explore the effect of photoisomerization on the supramolecular polymerization of **1c**, UV irradiation of the steady-state heptane solution ($c = 2 \times 10^{-4}$ M, average aggregate size is 150 nm) was followed by DLS and UV/Vis measurements. Figure 8 shows the changes in aggregate size and *cis/trans* ratio upon UV irradiation. Interestingly, the first

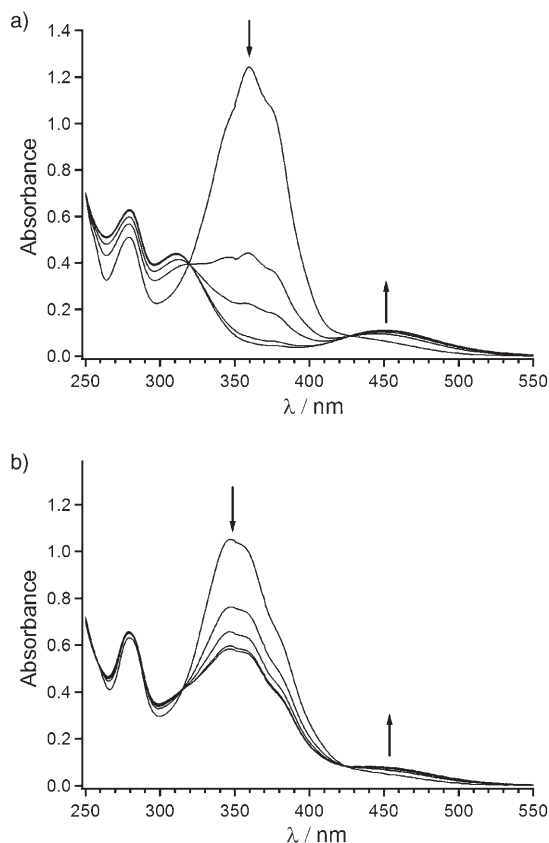


Figure 7. UV/Vis spectral changes (upon irradiation with 350 nm light) of solutions of **1c** ($c = 2 \times 10^{-5}$ M) in a) THF (0, 1, 2, 6 and 10 min), and b) heptane (0, 1, 2, 4, and 10 min).

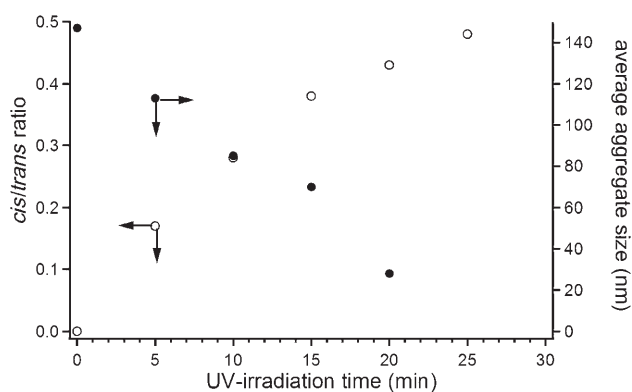


Figure 8. Changes in the *cis/trans* ratio of the azobenzene moiety (left axis, open circles) and the DLS-determined average aggregate size of **1c** (right axis, closed circles) in heptane ($c = 2 \times 10^{-4}$ M) versus irradiation time (350-nm light). The average aggregate size after irradiation for 25 min could not be measured because of the low scattering intensity.

20 min irradiation resulted in the dramatic diminution of the aggregate size, to roughly 30 nm, with an increase in the *cis/trans* ratio to 0.43. Further irradiation achieved a PS state (*cis/trans* ratio = 0.48), but the light scattering intensity in DLS measurement was too weak to be detectable by our DLS instrument, so we were not able to judge directly

whether the photoirradiation had induced complete disruption of the supramolecular polymers into the monomeric state. In view of the low *cis/trans* ratio (0.48) in the PS state, however, **1c** molecules in the PS state seem to remain aggregated.

Irradiation of the UV-irradiated solution with visible light (450 nm) rapidly restored a *trans*-rich PS state (*cis/trans* ratio = 0.90), within 5 min. DLS analysis showed the recovery of the aggregated species with an average size of 30 nm, and this again grew further with time, as in the case of the freshly prepared heptane solution of **1c** (vide supra). The original aggregate size (ca. 150 nm) recovered within 24 h, so the supramolecular polymerization of **1c** under dilute conditions is a photoreversible process. Figure 9 shows a molecular modeling-derived hexadecamer of **1c**, with one azobenzene moiety adopting a *cis* conformation (*trans,cis-1c*).

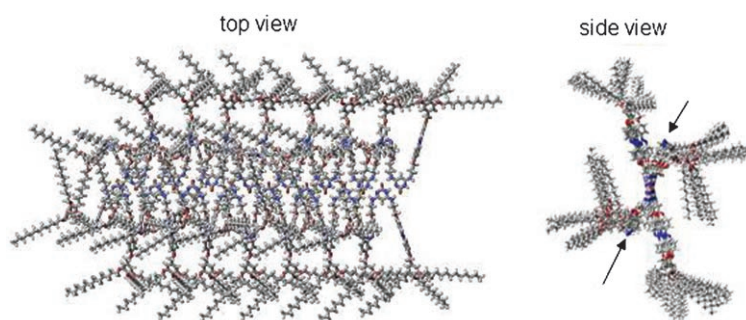


Figure 9. Molecular modeling-derived structure of hexadecameric **1c**, one azobenzene moiety of which is adopting the *cis* conformation (*trans,cis-1c*). Arrows indicate the *cis*-azobenzene moieties.

1c). While force-field calculations showed the hydrogen-bond-directed polymerization of *trans,cis-1c* to be an energetically favorable process, the resulting supramolecular tape lacks the crowding of the aliphatic tails contributing to the stabilization of the tape through van der Waals interaction. Thus, under relatively dilute conditions, as in this DLS experiment ($c = 2 \times 10^{-4} \text{ M}$), the degree of polymerization may decrease with the *trans* \rightarrow *cis* isomerization of the azobenzene side chains.

The azobenzene moieties of **1c** are highly photoreactive even in the organogel state. Figure 10 shows the changes undergone by the heptane gels of **1c** ($c = 1 \times 10^{-2} \text{ M}$) in 1-mm (a \rightarrow b) and 1-cm cuvettes (c \rightarrow d) upon UV light irradiation (150-W xenon lamp, 350 nm, bandwidth = 20 nm). The irradiation slowly dissolved macroscopic aggregates, resulting in the collapse of the gel within 1 h in the 1 mm cuvette and in 4 h in the 1-cm cuvette.^[19–21] The *cis/trans* ratio was roughly 0.4, as estimated from UV/Vis measurement upon 1000-fold dilution, indicating that one of the two azobenzene side chains of **1c** photoisomerized. DLS analysis of the photogenerated sol phase showed the presence of large aggregated species with the average size of 188 nm. These findings indicate that the *trans* \rightarrow *cis* isomerization of the azobenzene moieties induces the collapse of the lamellar structures into soluble supramolecular tapes (see XRD study described

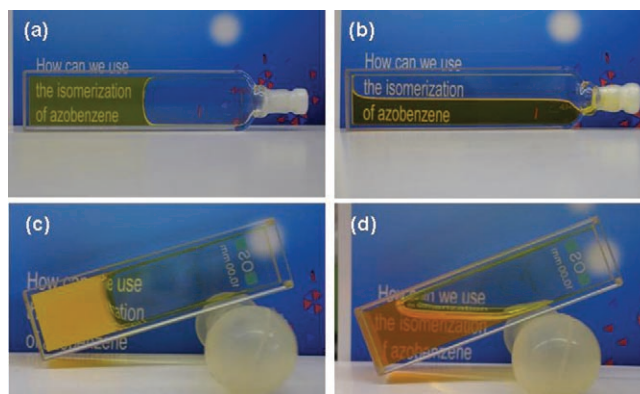


Figure 10. Photoinduced collapse of the heptane gel of **1c** ($c = 1 \times 10^{-2} \text{ M}$) in a 1-mm cuvette (a \rightarrow b, 1 h) and in a 1-cm cuvette (c \rightarrow d, 4 h) upon irradiation with 350-nm light.

below). Prolonged irradiation did not cause further disruption of the polymeric species, as judged from the DLS analysis. The persistence of the polymeric species in the PS state is convincing in view of the high concentration of **1c** ($c = 1 \times 10^{-2} \text{ M}$), which increases the degree of polymerization.

The cast films of the above photogenerated sol phases showed neither fibrous nor sheet-like structures on FE-SEM observation (Figure 11).

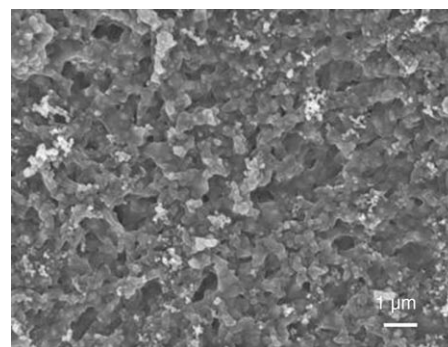


Figure 11. FE-SEM image of the cast film of the photogenerated heptane sol of **1c**.

The absence of extended lamellar structure was shown by POM and XRD analyses: the resulting film showed neither birefringence between crossed polarizers nor defined XRD peaks characteristic of the lamellar structure (Figure 12). Noteworthy here is that the weak diffraction peak at 9.59 Å corresponding to the periodic distance of the dimeric DAP units persists, demonstrating that the photogenerated sol phase indeed contains supramolecular tapes consisting of

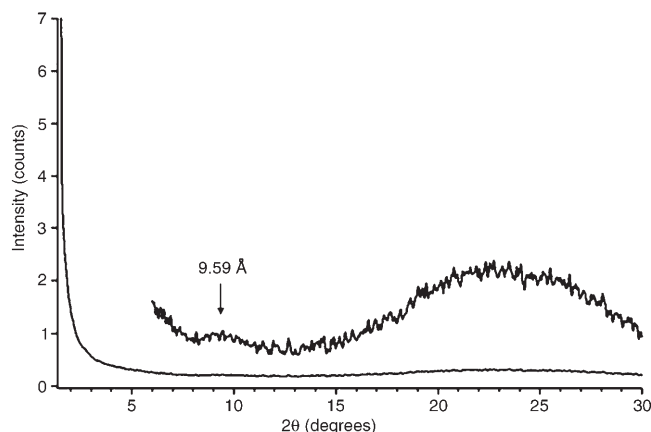


Figure 12. X-ray diffraction pattern of the cast film prepared from the photogenerated heptane sol of **1c**.

photoisomerized **1c** (i.e., *trans,cis-1c*). This is in agreement with the DLS result that showed the presence of polymeric species in the photogenerated sol phase. However, such supramolecular tapes contain roughly 40% of *cis*-azobenzene side chains as judged from the *cis/trans* ratio of 0.4, they might be randomly deposited on the surface in the air-drying process because of their unfavorable morphologies for the hierarchical organization. The molecular modeling-derived hexadecamer constructed from *trans,cis-1c* shown in Figure 9 again represents one of these morphologies well: the tridodecyloxyphenyl substituents attached to the *cis*-azobenzene moieties fully cover the aromatic surface of the supramolecular tapes. Obviously, such a morphology is unfavorable for extended stacking, so it can be concluded that the photoirradiation of the extended lamellar structures composed of stacked supramolecular tapes of **1c** resulted in the disruption of the lamellar structures into soluble supramolecular tapes (from left to right in Figure 13).

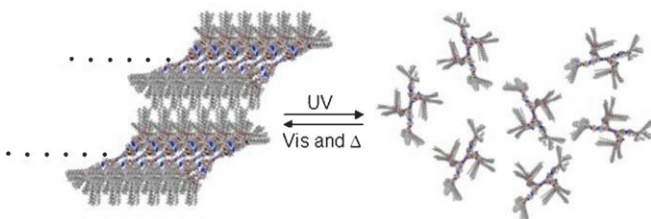


Figure 13. Schematic representation of the photoresponsive hierarchical organization for the supramolecular tapes (side views).

The UV-generated sol phase restored the original gel state (lamellar superstructures) upon irradiation with visible light (450 nm) and subsequent standing over 24 h (from right to left in Figure 13). This process includes photochemical *cis*→*trans* isomerization followed by the slow hierarchical association of the supramolecular tapes into extended lamellar structures. Photochemical gel→sol conversion and subsequent reformation of gel could be repeated at least five times without decomposition of **1c**.

Conclusion

Self-assembling building blocks that are readily functionalizable and capable of forming desired superstructures in solution and in the solid state are of great importance for the creation of functional nanomaterials. Herein, we have demonstrated the functionalization of *N,N'*-disubstituted 4,6-diaminopyrimidin-2(1*H*)-one (DAP), a versatile supramolecular building block for the creation of functional supramolecular polymers, using azobenzene photoresponsive side chains. The resulting functional DAP building blocks formed tapelike supramolecular polymers in nonpolar media, and these hierarchically organize into lamellar superstructures to form fiber- and sheet-like macroscopic entities. An especially interesting aspect of this compound is its photoresponse in the polymeric state, allowing photoinduced disruption and reformation of the lamellar superstructures in heptane, as demonstrated by the photochemically reversible sol–gel transition. We are now investigating the application of these photoresponsive supramolecular polymers in photopatterning techniques.^[20] Furthermore, several DAP derivatives possessing optoelectronically active substituents appear to show the versatility of DAP supramolecular building block as novel functional nanomaterials.

Experimental Section

General: ¹H NMR spectra were recorded on a JEOL LA400 spectrometer, and chemical shifts are reported in ppm with the TMS signal as internal standard. Variable-temperature ¹H NMR spectra were recorded on a JEOL LA500 spectrometer, and chemical shifts are reported in ppm with the signals of residual solvents as internal standard. UV spectra were measured on a JASCO V570 spectrophotometer, FAB-MS spectra on a JEOL JMS-AX500 mass spectrometer. Elemental analyses were performed at the Analytical Center of Chiba University. Electron microscopic observation was carried out by field emission scanning electron microscopy (JEOL JSM-6330F). The freeze-dried gels were sputtered with Os by use of a Meiwaofosis Neoc Pure Osmium Coater. Dynamic light scattering measurements were conducted on a Beckmann Coulter N5 particle analyzer fitted with a 25-mW He-Ne laser. The hot sample solutions were filtered with Millipore membrane filter (pore size = 0.2 μm) before measurements to remove dust. Photoirradiation experiments were performed on a fluorimeter fitted with a 150-W xenon lamp (20 nm excitation bandwidth). Molecular modeling calculations were performed with MacroModel version 9.0. MMFF force field calculation was applied for minimization of the hexadecamer of **1c** (solvent: chloroform). For the use of this calculation method, the conformation of the two phenyl rings in the azobenzene unit was constrained to coplanar with respect to the –N=N– double bond as obtained by MM2 calculation.

Compound **7** was prepared by the previously reported procedures.^[12] Column chromatography was performed on 63–210 μm silica gel. The solvents for the spectroscopic measurements and the gelling experiments were all spectral grade and were used without further purification. All other commercially available reagents and solvents were of reagent grade and were used without further purification.

***N*-[3-(4-Nitrophenoxy)propyl]phthalimide (2):** *N*-(3-Bromopropyl)phthalimide (5.78 g, 21.5 mmol) in dry DMF (15 mL) was added dropwise at 65°C under N₂ to a mixture of *p*-nitrophenol (3.0 g, 21.5 mmol) and K₂CO₃ (6.0 g) in dry DMF (15 mL) and the resulting mixture was stirred for 4 h. The mixture was cooled to room temperature and poured into ice water. The resulting precipitate was collected and used for the next step

without purification (6.8 g, 96.4% yield). ¹H NMR (400 MHz, CDCl₃): δ = 8.15 (d, *J* = 9.5 Hz, 2H), 7.85 (m, 2H), 7.74 (m, 2H), 6.85 (d, *J* = 9.3 Hz, 2H), 4.12 (t, *J* = 6.1 Hz, 2H), 3.93 (t, *J* = 6.8 Hz, 2H), 2.24 (q, *J* = 6.6 Hz, 2H) ppm; MS (FAB): 327 [M]⁺.

4-[4-[(3-Phthalimidopropyl)oxy]phenylazo]phenol (4): A mixture of compound **2** (2.5 g, 7.66 mmol) and Pd/C (250 mg) in dry THF was stirred at 65°C under H₂ for 24 h. The mixture was filtered and the filtrate was evaporated to dryness. The residue was purified by column chromatography on silica gel (hexane/ethyl acetate 1:5) to give the corresponding aniline derivative **3** (1.78 g, 78.4% yield). The entire product was dissolved in acetone/water (1:1 mixture) and conc. HCl (2 mL) was added to the mixture at 0°C. NaNO₂ (450 mg) in water (7 mL) was added to this solution, and the mixture was stirred for 15 min at 0°C. This solution was slowly added to an aqueous solution (20 mL) of phenol (611 mg) containing NaOH (390 mg) and Na₂CO₃ (1.0 g). The resulting red precipitates were collected by filtration to give crude compound **4** (1.7 g). This compound was used for following etherification without further purification. ¹H NMR (400 MHz, CDCl₃): δ = 7.85 (m, 2H), 7.81 (m, 4H), 7.72 (m, 2H), 6.92 (d, *J* = 9.0 Hz, 2H), 6.86 (d, *J* = 9.0 Hz, 2H), 4.11 (t, *J* = 6.1 Hz, 2H), 3.95 (t, *J* = 6.1 Hz, 2H), 2.23 (q, *J* = 6.4 Hz, 2H) ppm.

General procedure for the preparation of compounds 5a–c: The chlorinated compound (1.24 mmol) in dry DMF (15 mL) was added dropwise at 65°C under N₂ to a mixture of compound **4** (1.24 mmol) and K₂CO₃ (4.0 g) in dry DMF (15 mL), and the resulting mixture was stirred for 4 h. The mixture was cooled to room temperature and poured into ice water. The resulting yellow precipitates were collected and purified by column chromatography over silica gel with chloroform as eluent to give compounds **5a–c**.

4-Dodecyloxy-1-[4-[(3-phthalimidopropyl)oxy]phenylazo]benzene (5a, 79% yield): ¹H NMR (400 MHz, CDCl₃): δ = 7.85 (m, 2H), 7.85 (d, *J* = 9.0 Hz, 2H), 7.82 (d, *J* = 9.0 Hz, 2H), 7.73 (m, 2H), 6.98 (d, *J* = 9.0 Hz, 2H), 6.88 (d, *J* = 9.0 Hz, 2H), 4.11 (t, *J* = 6.1 Hz, 2H), 4.03 (t, *J* = 6.6 Hz, 2H), 3.94 (t, *J* = 6.8 Hz, 2H), 2.22 (m, 2H), 1.81 (q, *J* = 8.1 Hz, 2H), 1.57 (m, 2H), 1.26 (m, 16H), 0.88 (m, 3H) ppm; MS (FAB): 571 [M+H]⁺.

4-[(2-Ethylhexyl)oxy]-1-[4-[(3-phthalimidopropyl)oxy]phenylazo]benzene (5b, 83% yield): ¹H NMR (400 MHz, CDCl₃): δ = 7.85 (m, 2H), 7.85 (d, *J* = 9.0 Hz, 2H), 7.82 (d, *J* = 9.0 Hz, 2H), 7.72 (m, 2H), 6.99 (d, *J* = 9.0 Hz, 2H), 6.88 (d, *J* = 9.0 Hz, 2H), 4.11 (t, *J* = 6.1 Hz, 2H), 3.93 (m, 4H), 2.23 (m, 2H), 1.75 (m, 1H), 1.55–1.31 (m, 8H), 0.93 (m, 6H) ppm; MS (FAB): 513 [M+H]⁺.

1-[4-[(3-Phthalimidopropyl)oxy]phenylazo]-4-[3,4,5-tris(dodecan-1-yloxy)benzyloxy]benzene (5c, 73% yield): ¹H NMR (400 MHz, CDCl₃): δ = 7.85 (m, 2H), 7.85 (d, *J* = 9.0 Hz, 2H), 7.82 (d, *J* = 9.0 Hz, 2H), 7.72 (m, 2H), 7.06 (d, *J* = 9.0 Hz, 2H), 6.88 (d, *J* = 9.0 Hz, 2H), 6.63 (s, 2H), 5.02 (s, 2H), 4.11 (t, *J* = 6.1 Hz, 2H), 3.95 (m, 8H), 2.23 (m, 2H), 1.77 (m, 6H), 1.55–1.31 (m, 48H), 0.88 (m, 9H) ppm; MS (FAB): 1045 [M+H]⁺.

General procedure for the preparation of compounds 6a–c: Mixtures of compounds **5a–5c** (0.9 mmol) and hydrazine monohydrate (0.4 mL) in ethanol (40 mL) were heated at reflux for 4 h. The mixture was extracted with CHCl₃ and the combined organic phases were washed with water, dried over Na₂SO₄, and evaporated to dryness to give compounds **6a–c** in almost pure states.

1-[4-[(3-Aminopropyl)oxy]phenylazo]-4-dodecyloxybenzene (6a, 99% yield): ¹H NMR (400 MHz, CDCl₃): δ = 7.86 (d, 4H), 6.99 (m, 4H), 4.13 (t, *J* = 6.1 Hz, 2H), 4.03 (t, *J* = 6.6 Hz, 2H), 2.94 (t, *J* = 6.8 Hz, 2H), 1.97 (q, *J* = 6.6 Hz, 2H), 1.81 (m, 2H), 1.47 (m, 2H), 1.34 (m, 16H), 0.88 (m, 3H) ppm; MS (FAB): 860 [M+H]⁺.

1-[4-[(3-Aminopropyl)oxy]phenylazo]-4-[(2-ethylhexyl)oxy]benzene (6b, 98% yield): ¹H NMR (400 MHz, CDCl₃): δ = 7.86 (d, 4H), 6.99 (d, 4H), 4.13 (t, *J* = 6.4 Hz, 2H), 3.92 (d, *J* = 5.6 Hz, 2H), 2.94 (t, *J* = 6.8 Hz, 2H), 1.97 (m, 2H), 1.76 (m, 1H), 1.56–1.25 (m, 8H), 0.93 (m, 6H) ppm; MS (FAB): 860 [M+H]⁺.

1-[4-[(3-Aminopropyl)oxy]phenylazo]-4-[3,4,5-tris(*n*-dodecan-1-yloxy)benzyloxy]benzene (6c, 99% yield): ¹H NMR (400 MHz, CDCl₃): δ = 7.87 (m, 4H), 7.07 (d, *J* = 9.0 Hz, 2H), 7.00 (d, *J* = 9.3 Hz, 2H), 7.06 (d,

J = 9.0 Hz, 2H), 6.63 (s, 2H), 5.02 (s, 2H), 4.14 (t, *J* = 6.3 Hz, 2H), 3.95 (m, 6H), 2.94 (t, *J* = 6.6 Hz, 2H), 1.97 (m, 2H), 1.77 (m, 6H), 1.55–1.31 (m, 48H), 0.88 (m, 9H) ppm; MS (FAB): 860 [M+H]⁺.

General procedures for compounds 1a–c: Mixtures of **6a–c** (0.43 mmol), the sodium salt of 4,6-dichloropyrimidin-2(1*H*)-one (0.21 mmol), and diisopropylethylamine (0.3 mL) in dry dioxane (20 mL) were stirred at 105°C for 24 h. The mixture was cooled to room temperature and poured into ice water and extracted with CHCl₃. The combined organic phase was dried over Na₂SO₄ and concentrated to dryness. The residue was dissolved in CHCl₃ and adsorbed on silica gel. First, a mixture of ethyl acetate/methanol 9:1 was used as eluent to remove by-products, and the desired compound was then eluted with chloroform/methanol 20:1. Compounds **1a** and **1b** could not be purified to completely pure states because of their low solubilities in organic solvents.

***N,N*-Bis[3-(4-[4-[3,4,5-tris(*n*-dodecan-1-yloxy)benzyloxy]phenylazo]phenoxy)propyl]-4,6-diaminopyrimidin-2(1*H*)-one (1c, 61% yield):** ¹H NMR (400 MHz, CDCl₃): δ = 7.80 (m, 8H), 7.00 (d, *J* = 9.0 Hz, 4H), 6.91 (d, *J* = 8.3 Hz, 4H), 6.61 (s, 4H), 4.95 (s, 4H), 4.55 (s, 1H), 3.94 (m, 16H), 3.17 (br, 4H), 1.98 (br, 4H), 1.76 (m, 12H), 1.44 (m, 12H), 1.25 (m, 96H), 0.88 (m, 18H) ppm; MS (FAB): 1922 [M+H]⁺; elemental analysis (%) calcd for C₁₂H₁₉₀N₈O₁₁: C 75.03, H 9.97, N 5.83, O 9.16; found: C 74.85, H 9.77, N 5.80.

Acknowledgements

This work was partially supported by a Grant-in-Aid for Young Scientists (B) (No. 17750120) from the Ministry of Education, Culture, Sports, Science and Technology. S. Y. thanks Iketani Science and Technology Foundation for the financial support.

- Reviews of supramolecular polymers, see: a) T. Kato, *Supramol. Sci.* **1996**, *3*, 53–59; b) J. S. Moore, *Curr. Opin. Colloid Interface Sci.* **1999**, *4*, 108–116; c) M. J. Krische, J.-M. Lehn, *Struct. Bonding (Berlin)* **2000**, *94*, 3–29; d) T. Kato, *Struct. Bonding (Berlin)* **2000**, *96*, 95–146; e) L. Brunsveld, B. J. B. Folmer, R. P. Sijbesma, E. W. Meijer, *Chem. Rev.* **2001**, *101*, 4071–4098; f) T. Kato, N. Mizoshita, K. Kanie, *Macromol. Rapid Commun.* **2001**, *22*, 797–814; g) A. T. ten Cate, R. P. Sijbesma, *Macromol. Rapid Commun.* **2002**, *23*, 1094–1112; h) A. Ciferri, *Macromol. Rapid Commun.* **2002**, *23*, 511–529; i) J.-M. Lehn, *Polym. Int.* **2002**, *35*, 825–839; j) J.-F. Gohy, B. G. G. Lohmeijer, U. S. Schubert, *Chem. Eur. J.* **2003**, *9*, 3472–3479; k) T. Kato, N. Mizoshita, K. Kishimoto, *Angew. Chem.* **2006**, *118*, 44–74; *Angew. Chem. Int. Ed.* **2006**, *45*, 38–68.
- F. J. M. Hoeben, P. Jonkheijm, E. W. Meijer, A. P. H. J. Schenning, *Chem. Rev.* **2005**, *105*, 1491–1546.
- Reviews of multiple hydrogen-bonding interactions, see: a) G. M. Whitesides, E. E. Simanek, J. P. Mathias, C. T. Seto, D. Chin, M. Mammen, D. M. Gordon, *Acc. Chem. Res.* **1995**, *28*, 37–44; b) K. Ariga, T. Kunitake, *Acc. Chem. Res.* **1998**, *31*, 371–378; c) C. Schmuck, W. Wienand, *Angew. Chem.* **2001**, *113*, 4493–4499; *Angew. Chem. Int. Ed.* **2001**, *40*, 4363–4369; d) D. C. Sherrington, K. A. Taskinen, *Chem. Soc. Rev.* **2001**, *30*, 83–93; e) R. P. Sijbesma, E. W. Meijer, *Chem. Commun.* **2003**, 5–16.
- For examples of supramolecular polymers based on DNA-base-type multiple hydrogen-bonding interactions: a) C. Fouquey, J.-M. Lehn, A.-M. Levelut, *Adv. Mater.* **1990**, *2*, 254–257; b) T. Gulik-Krzywicki, C. Fouquey, J.-M. Lehn, *Proc. Natl. Acad. Sci. USA* **1993**, *90*, 163–167; c) M. Kotera, J.-M. Lehn, J.-P. Vigneron, *J. Chem. Soc. Chem. Commun.* **1994**, 197–199; d) R. P. Sijbesma, F. H. Beijer, L. Brunsveld, B. J. B. Folmer, J. H. K. K. Hirschberg, R. F. M. Lange, J. K. L. Lowe, E. W. Meijer, *Science* **1997**, *278*, 1601–1604; e) J. H. K. K. Hirschberg, L. Brunsveld, A. Ramzi, J. A. J. M. Vekemans, R. P. Sijbesma, E. W. Meijer, *Nature* **2000**, *407*, 167–170; f) V. Berl, M. Schmutz, M. J. Krische, R. G. Khoury, J.-M. Lehn, *Chem. Eur. J.* **2002**, *8*, 1227–1244; g) J. H. K. K. Hirschberg, R. A. Koevoets, R. P.

- Sijbesma, E. W. Meijer, *Chem. Eur. J.* **2003**, *9*, 4222–4231; h) S. Yagai, M. Higashi, T. Karatsu, A. Kitamura, *Chem. Mater.* **2004**, *16*, 3582–3585; i) M. Ikeda, T. Nobori, M. Schmutz, J.-M. Lehn, *Chem. Eur. J.* **2005**, *11*, 662–668.
- [5] For pioneering works on hydrogen-bonded supramolecular polymer liquid crystals, see: a) T. Kato, J. M. J. Fréchet, *J. Am. Chem. Soc.* **1989**, *111*, 8533–8534; b) T. Kato, J. M. J. Fréchet, *Macromolecules* **1989**, *22*, 3818–3819; c) T. Kato, H. Kihara, U. Kumar, T. Uryu, J. M. J. Fréchet, *Angew. Chem.* **1994**, *106*, 1728–1730; *Angew. Chem. Int. Ed. Engl.* **1994**, *33*, 1644–1645; d) H. Kihara, T. Kato, T. Uryu, J. M. J. Fréchet, *Chem. Mater.* **1996**, *8*, 961–968.
- [6] a) N. Kimizuka, S. Fujikawa, H. Kuwahara, T. Kunitake, A. Marsh, J.-M. Lehn, *J. Chem. Soc. Chem. Commun.* **1995**, 2103–2104; b) N. Kimizuka, T. Kawasaki, K. Hirata, T. Kunitake, *J. Am. Chem. Soc.* **1995**, *117*, 6360–6361; c) G. Gottarelli, E. Mezzina, G. P. Spada, F. Carsughi, G. Di Nicola, P. Mariani, A. Sabatucci, S. Bonazzi, *Helv. Chim. Acta* **1996**, *79*, 220–234; d) W. Yang, X. Chai, Y. Tian, S. Chen, Y. Cao, R. Lu, Y. Jiang, T. Li, *Liq. Cryst.* **1997**, *22*, 579–583; e) M. Suárez, J.-M. Lehn, S. C. Zimmerman, A. Skoulios, B. Heinrich, *J. Am. Chem. Soc.* **1998**, *120*, 9526–9532; f) W. Yang, X. Chai, Y. Tian, S. Chen, Y. Cao, R. Lu, Y. Jiang, T. Li, *Chem. Eur. J.* **1999**, *5*, 1144–1149; g) H.-A. Klok, K. A. Jolliffe, C. L. Schauer, L. J. Prins, J. P. Spatz, M. Möller, P. Timmerman, D. N. Reinhoudt, *J. Am. Chem. Soc.* **1999**, *121*, 7154–7155; h) I. S. Choi, X. Li, E. E. Simanek, R. Akaba, G. M. Whitesides, *Chem. Mater.* **1999**, *11*, 648–690; i) L. Brunsveld, H. Zhang, M. Glasbeek, J. A. J. M. Vekemans, E. W. Meijer, *J. Am. Chem. Soc.* **2000**, *122*, 6175–6182; j) M. Enomoto, A. Kishimura, T. Aida, *J. Am. Chem. Soc.* **2001**, *123*, 5608–5609; k) H. Fenniri, P. Mathivanan, K. L. Vidale, D. M. Sherman, K. Hallenga, K. V. Wood, J. G. Stowell, *J. Am. Chem. Soc.* **2001**, *123*, 3854–3855; l) T. Giorgi, S. Lena, P. Mariani, M. A. Cremonini, S. Masiero, S. Pieraccini, J. P. Rabe, P. Samori, G. P. Spada, G. Gottarelli, *J. Am. Chem. Soc.* **2003**, *125*, 14741–14749; m) J. Barbera, E. Caverio, M. Lehmann, J.-L. Serrano, T. Sierra, J. T. Vazquez, *J. Am. Chem. Soc.* **2003**, *125*, 4527–4533; n) P. Jonkheijm, A. Miura, M. Zdanowska, F. J. M. Hoeben, S. De Feyter, A. P. H. J. Schenning, F. C. De Schryver, E. W. Meijer, **2003**, *116*, 76–80; *Angew. Chem.* **2004**, *116*, 76–80; *Angew. Chem. Int. Ed.* **2004**, *43*, 74–79; o) Y. Kamikawa, M. Nishii, T. Kato, *Chem. Eur. J.* **2004**, *10*, 5942–5951; p) S. Jin, Y. Ma, S. C. Zimmerman, S. Z. D. Cheng, *Chem. Mater.* **2004**, *16*, 2975–2977; q) J. Barbera, L. Puig, J. L. Serrano, T. Sierra, *Chem. Mater.* **2004**, *16*, 3308–3317; r) J. Barbera, L. Puig, P. Romero, J. L. Serrano, T. Sierra, *J. Am. Chem. Soc.* **2005**, *127*, 458–464; s) J. G. Morales, J. Raez, T. Yamazaki, R. K. Motkuri, A. Kovalenko, H. Fenniri, *J. Am. Chem. Soc.* **2005**, *127*, 8307–8309; t) S. Yagai, T. Nakajima, K. Kishikawa, S. Kohmoto, T. Karatsu, A. Kitamura, *J. Am. Chem. Soc.* **2005**, *127*, 11134–11139; u) S. Yagai, M. Higashi, T. Karatsu, A. Kitamura, *Chem. Mater.* **2005**, *17*, 4392–4398.
- [7] Lamellar structures generated from guanine derivatives: a) G. Gottarelli, G. P. Spada, *Chem. Rec.* **2004**, *4*, 39–49; b) T. Giorgi, F. Grepioni, I. Manet, P. Mariani, S. Masiero, E. Mezzina, S. Pieraccini, L. Saturni, G. P. Spada, G. Gottarelli, *Chem. Eur. J.* **2002**, *8*, 2143–2152; c) G. Gottarelli, S. Masiero, E. Mezzina, S. Pieraccini, J. P. Rabe, P. Samori, G. P. Spada, *Chem. Eur. J.* **2000**, *6*, 3242–3248; d) G. Maruccio, P. Visconti, V. Arima, S. D'Amico, A. Biasco, E. D'Amone, R. Cingolani, R. Rinaldi, S. Masiero, T. Giorgi, G. Gottarelli, *Nano Lett.* **2003**, *3*, 479–483.
- [8] Lamellar structures generated from folic acid derivatives: a) T. Kato, *Science* **2002**, *295*, 2414–2418; b) K. Kanie, M. Nishii, T. Yasuda, T. Taki, S. Ujiie, T. Kato, *J. Mater. Chem.* **2001**, *11*, 2875–2886; c) K. Kanie, T. Yasuda, M. Nishii, S. Ujiie, T. Kato, *Chem. Lett.* **2001**, 480–481; d) K. Kanie, T. Yasuda, S. Ujiie, T. Kato, *Chem. Commun.* **2000**, 1899–1900.
- [9] Reviews of photoresponsive self-assemblies: a) S. Yagai, T. Karatsu, A. Kitamura, *Chem. Eur. J.* **2005**, *11*, 4054–4063; b) S. Hecht, *Small* **2005**, *1*, 26–29; c) C.-H. Huang, D. M. Bassani, *Eur. J. Org. Chem.* **2005**, 4041–4050.
- [10] Selected examples of photoresponsive self-assembly: a) M. S. Vollmer, T. D. Clark, C. Steinem, M. R. Ghadiri, *Angew. Chem.* **1999**, *111*, 1703–1706; *Angew. Chem. Int. Ed.* **1999**, *38*, 1598–1601; b) X. Liang, H. Asanuma, M. Komiyama, *J. Am. Chem. Soc.* **2002**, *124*, 1877–1883; c) S. Yagai, T. Karatsu, A. Kitamura, *Chem. Commun.* **2003**, 1844–1845; d) F. Rakotondrandany, M. A. Whitehead, A.-M. Lebuis, H. F. Sleiman, *Chem. Eur. J.* **2003**, *9*, 4771–4780; e) S. Yagai, T. Nakajima, T. Karatsu, K.-i. Saitow, A. Kitamura, *J. Am. Chem. Soc.* **2004**, *126*, 11500–11508; f) Y. Molard, D. M. Bassani, J.-P. Desvergne, P. N. Horton, M. B. Hursthouse, J. H. R. Tucker, *Angew. Chem.* **2005**, *117*, 1096–1099; *Angew. Chem. Int. Ed.* **2005**, *44*, 1072–1075; g) M. Takeshita, M. Hayashi, S. Kadota, K. H. Mohammed, T. Yamato, *Chem. Commun.* **2005**, 761–763.
- [11] Supramolecular tapes composed of melamine and cyanurate or barbiturate components: a) J. A. Zerkowski, J. C. MacDonald, C. T. Seto, D. A. Wierda, G. M. Whitesides, *J. Am. Chem. Soc.* **1994**, *116*, 2382–2391; b) K. Hanabusa, T. Miki, Y. Taguchi, T. Koyama, H. Shirai, *J. Chem. Soc. Chem. Commun.* **1993**, 1382–1384; c) N. Kimizuka, T. Kawasaki, T. Kunitake, *J. Am. Chem. Soc.* **1993**, *115*, 4387–4388; d) N. Kimizuka, T. Kawasaki, K. Hirata, T. Kunitake, *J. Am. Chem. Soc.* **1998**, *120*, 4094–4104; e) T. Kawasaki, M. Tokunishi, N. Kimizuka, T. Kunitake, *J. Am. Chem. Soc.* **2001**, *123*, 6792–6800; f) H. Koyano, P. Bissel, K. Yoshihara, K. Ariga, T. Kunitake, *Chem. Eur. J.* **1997**, *3*, 1077–1082; g) F. Würthner, S. Yao, B. Heise, C. Tschierske, *Chem. Commun.* **2001**, 2260–2261; h) M. Mascal, J. Hansen, P. S. Fallon, A. J. Blake, B. R. Heywood, M. H. Moore, J. P. Turkenburg, *Chem. Eur. J.* **1999**, *5*, 381–384.
- [12] S. Yagai, T. Iwashima, T. Karatsu, A. Kitamura, *Chem. Commun.* **2004**, 1114–1115.
- [13] J.-M. Lehn, M. Mascal, A. DeCian, J. Fischer, *J. Chem. Soc. Perkin Trans. 2* **1992**, 461–467.
- [14] a) T. Kunitake, N. Nakashima, M. Shimomura, Y. Okahata, K. Kano, T. Ogawa, *J. Am. Chem. Soc.* **1980**, *102*, 6642–6644; b) H. Sakai, A. Matsumura, S. Yokoyama, T. Saji, M. Abe, *J. Phys. Chem. B* **1999**, *103*, 10737–10740; c) C. G. Morgan, E. W. Thomas, S. S. Sandhu, Y. P. Yianni, A. C. Mitchell, *Biochim. Biophys. Acta* **1987**, *903*, 504–509; d) X. Song, J. Perlstein, D. G. Whitten, *J. Am. Chem. Soc.* **1997**, *119*, 9144–9159; e) D. G. Whitten, L. Chen, H. C. Geiger, J. Perlstein, X. Song, *J. Phys. Chem. B* **1998**, *102*, 10098–10111; f) J. M. Kuiper, J. B. F. N. Engberts, *Langmuir* **2004**, *20*, 1152–1160.
- [15] Reviews for organogels, see: a) P. Terech, R. G. Weiss, *Chem. Rev.* **1997**, *97*, 3133–3160; b) D. J. Abdallah, R. G. Weiss, *Adv. Mater.* **2000**, *12*, 1237–1247; c) J. H. van Esch, B. L. Feringa, *Angew. Chem.* **2000**, *112*, 2351–2354; *Angew. Chem. Int. Ed.* **2000**, *39*, 2263–2266.
- [16] C. Tschierske, *J. Mater. Chem.* **1998**, *8*, 1485–1508.
- [17] Micro-segregation has been suggested for liquid crystalline hydrogen-bonded tapelike assemblies: see References [7b, 11g].
- [18] a) L. Plasseraud, L. G. Cuervo, D. Guillon, G. S.-Fink, R. Descheaux, D. W. Bruce, B. Donnio, *J. Mater. Chem.* **2002**, *12*, 2653–2658; b) N. Laurent, D. Lafont, F. Dumoulin, P. Boullanger, G. Mackenzie, P. H. J. Kouwer, J. W. Goodby, *J. Am. Chem. Soc.* **2003**, *125*, 15499–15506.
- [19] Photoresponsive organogels: a) J. Eastoe, M. Sánchez-Dominguez, P. Wyatt, R. K. Heenan, *Chem. Commun.* **2004**, 2608–2609; b) J. J. D. de Jong, L. N. Lucas, R. M. Kellogg, J. H. van Esch, B. L. Feringa, *Science* **2004**, *304*, 278–281; c) J. J. D. de Jong, P. R. Hania, A. Pugžlys, L. N. Lucas, M. de Loos, R. M. Kellogg, B. L. Feringa, K. Duppen, J. H. van Esch, *Angew. Chem.* **2005**, *117*, 2425–2428; *Angew. Chem. Int. Ed.* **2005**, *44*, 2373–2376; d) N. Koumura, M. Kudo, N. Tamaoki, *Langmuir* **2004**, *20*, 9897–9900; e) K. Murata, M. Aoki, T. Nishi, A. Ikeda, S. Shinkai, *J. Chem. Soc. Chem. Commun.* **1991**, 1715–1718; f) K. Murata, M. Aoki, T. Suzuki, T. Harada, H. Kawabata, T. Komori, F. Ohseto, K. Ueda, S. Shinkai, *J. Am. Chem. Soc.* **1994**, *116*, 6664–6676; g) S. A. Ahmed, X. Sallenne, F. Fages, G. Mieden-Gundert, W. M. Müller, U. Müller, F. Vögtle, J.-L. Pozzo, *Langmuir* **2002**, *18*, 7096–7101; h) L. Frkanec, M. Jokic, J. Makarevič, K. Wolsperger, M. Zinic, *J. Am. Chem. Soc.* **2002**, *124*, 9716–9717; i) S. van der Laan, B. L. Feringa, R. M. Kellogg, J. H. van Esch, *Langmuir* **2002**, *18*, 7136–7140; j) M. Ayabe, T. Kishida, N. Fujita, K. Sada, S. Shinkai, *Org. Biomol. Chem.* **2003**, *1*, 2744–2747.

- [20] Photoresponsive liquid crystalline gels: a) M. Moriyama, N. Mizoshita, T. Yokota, K. Kishimoto, T. Kato, *Adv. Mater.* **2003**, *15*, 1335–1338; b) Y. Zhao, X. Tong, *Adv. Mater.* **2003**, *15*, 1431–1435.
- [21] Photoisomerization of the azobenzene moieties in several azobenzene-incorporated organogel systems has been suppressed by strong *H*-type aggregation, see: a) D. Inoue, M. Suzuki, H. Shirai, K. Hanabusa, *Bull. Chem. Soc. Jpn.* **2005**, *78*, 721–726; b) S. Yagai, T. Karatsu, A. Kitamura, *Langmuir* **2005**, *21*, 11048–11052.

Received: November 26, 2005

Revised: February 3, 2006

Published online: March 21, 2006